Modelling the chemical recycling of crosslinked poly (methyl methacrylate): kinetics of depolymerisation

Simoní Da Ros [a*,1], Rayany Stocco Braido[a], Nathany Lisbôa de Souza e Castro[a], Amanda L. T. Brandão[b], Marcio Schwaab[c], José Carlos Pinto[a]

[a] Programa de Engenharia Química/COPPE, Universidade Federal do Rio de Janeiro, Cidade Universitária, CP:68502, Rio de Janeiro, 21941-972, RJ, Brazil.

[b] Departamento de Engenharia Química e de Materiais, Pontifícia Universidade Católica do Rio de Janeiro, 22451-900/38097, Brazil.

[c] Departamento de Engenharia Química, Universidade Federal do Rio Grande do Sul, Rua Engenheiro Luiz Englert, s/n - Prédio 12204, Porto Alegre, 90040-040, Brazil.

[*] Correspondence author

E-mail addresses: s.ros@ucl.ac.uk (correspondence author, S. Da Ros), rayany@peq.coppe.ufrj.br (R.S. Braido), nlisboa@eq.ufrj.br (N.L. de Souza e Castro), amanda.lemette@puc-rio.br (A. L. T. Brandão), schwaab@ufrgs.br (M. Schwaab), pinto@peq.coppe.ufrj.br (J. C. Pinto)

[1] Present address: Centre for Sustainable Heritage, University College London, 14 Upper Woburn Place, WC1H 0NN London, UK.

ABSTRACT:

Whereas increasing plastic solid waste production constitutes one of the main challenges of modern society, mainly due to the lack of suitable recycling technologies, chemical recycling represents an attractive solution for the conversion of plastic solid waste into valuable chemical intermediates. Herein, a kinetic model for the pyrolysis of a dental industry waste, ethylene glycol dimethacrylate (EGDMA) crosslinked poly (methyl methacrylate) (PMMA), is presented for the first time. Kinetics parameters and their statistical significance have been estimated from eight non-isothermal thermogravimetric analysis (TGA) experiments with heating rates varying between 5 and 50 °C·min^{-1} by using nonlinear regression. Our analysis indicates that the mechanism of depolymerisation of EGDMA crosslinked PMMA is likely to involve a consecutive reaction pathway involving two steps. The developed kinetic model - containing five kinetic parameters only - was able to predict well all non-isothermal TGA runs, and was validated against isothermal TGA experiments at 400 °C.

Keywords: plastic solid waste, chemical recycling, poly (methyl methacrylate), thermogravimetric analysis.

1. Introduction

Since the first semi-synthetic polymer discoveries in the late 19th century until the present day [1], plastics have revolutionised society by allowing the development of materials with the most diverse and unique properties, resulting in technological solutions with applications in a wide range of fields. Consequently, global plastic production has presented a remarkable rise, with figures ranging from 2 to 380 million metric tons (Mt) between 1950 and 2015 [2]. Concomitantly, global plastic solid waste production has also risen, totalling 150 Mt per year, whereas recycling rates have remained unsatisfactorily low [3]. For example, according to the Association of Plastics Manufactures in Europe and the European Association of Plastics Recycling and Recovery Organisations, from the 27.1 Mt of plastic waste collected in Europe in 2016, only 31.1% was recycled, while 41.6% was burnt for energy recovery and 27.3% were disposed in landfills [4].

Low recycling rates and increasing plastic solid waste production constitute one of the main challenges of modern society, mainly due to the lack of suitable recycling technologies [3]. In this context, chemical recycling (or tertiary recycling) represents an attractive alternative because it allows for the conversion of plastic solid waste into valuable chemical intermediates [5,6], thus contributing for the reduction of natural resources consumption and production of waste, while presenting potential for energy and monetary savings [3,7–9].

Poly (methyl methacrylate) (PMMA), is an industrially relevant polymer which finds unique applications, such as in its use in biomedical drug release systems, as optical fibers for light transmission, plastic eyeglass, contact lenses, denture materials, signs and displays, and liquid crystal displays (LCD) panels [7,10–12]. Due to its wide applicability, owing to its outstanding properties such as optical clarity, non-toxicity and resistance towards impact and most chemicals, PMMA demand is expected to grow over the coming years, with its market size projected to reach USD 8.16 billion by 2025, imposing a pressure on its average price,

which is already high when compared to common polymers, and increasing concerns on PMMA waste management [8,9].

In the dental industry, ethylene glycol dimethacrylate (EGDMA) cross-linked PMMA is used to produce artificial teeth for dentures manufacturing, by moulding polymer disks in teeth shaped moulds. Substantial PMMA waste is produced in this moulding step, resulting in considerable losses, Fig. 1.1(a).

The recycling of PMMA waste has been assessed by different methods, including its direct reuse in the production of new polymers [13] and asphalt mixtures [14], and its mechanical [9,15,16] and chemical [9,11,17–19] recycling. Whereas the direct reuse of PMMA waste usually requires clean and uncontaminated streams, its mechanical recycling may allow for the processing of waste streams containing other types of plastics, however it usually results in polymers with inferior properties [8,15]. In contrast, the chemical recycling of PMMA by thermal pyrolysis has demonstrated great potential for the recovery of the methyl methacrylate (MMA) monomer [11,17–19], which can be further polymerised to result in polymer resins presenting comparable properties to those obtained by using virgin and non-recycled monomer [17,18]. Additionally, the PMMA pyrolysis can be suggested as a robust process, as impurities, such as different resins, can be separated in the MMA purification step by distillation [17] and have been reported to result in no significant impact on the MMA recovery yield [9].

However, in order to allow for the design, control and optimisation of a thermal pyrolysis reactor, a model able to describe the kinetics of depolymerisation is necessary. From this, the optimal operational conditions for an economically feasible recycling process can be established. Indeed, the kinetics of PMMA depolymerisation has long been investigated, with several experimental evidences pointing towards the paramount importance of the polymer structure on the depolymerisation mechanism [7,20–24].

When MMA is polymerised via free radical polymerisation in the absence of chain-transfer agents, combination and disproportionation termination reactions may lead to the formation of head-to-head linkages and vinylidene end groups throughout the final polymer structure [20,22,23]. In contrast, MMA anionic polymerisation, or free radical polymerisation in the presence of chain-transfer agents, does not lead to significant amounts of these irregular groups in the resultant PMMA [21]. Additionally, the synthesis of PMMA by using crosslinking additives may result in a further distinct polymer matrix [19,25,26]. Thus, different reaction pathways have been proposed to explain the free radical depolymerisation reaction network involved in the PMMA degradation.

According to some authors, the degradation process can be initiated by the breakdown of head-to-head linkages followed by end chain scissions associated to vinylidene end groups, when these structures are present in the polymer matrix [20], as illustrated in Fig.1.1(b-c). The end chain scission could occur due to the breaking of a carbon-carbon bond β to the double bond, resulting in the formation of a monomer and a new vinylidene group in the remaining chain [20]. However, the above hypothesis has been contested, with the end chain scission initiation being explained by a radical transfer to the vinyl chain end instead [22], Fig.1.1(c). Regardless of the source of the radical, the dependence of this degradation step on the sample thickness has been demonstrated [22], supporting the role of radicals and their residence time within the polymer matrix. In the absence of irregular linkages, the degradation has been suggested to initiate by a random main chain scission process [20], Fig.1.1(d), although an initiation involving the homolytic scission of methoxycarbonyl side groups has also been supported [24]. Additionally, PMMA crosslinked with diallylmaleate and diallylphthalate has been suggested to depolymerise from the cross-linking points, whereas crosslinking with amines would favour random chain scission [25].
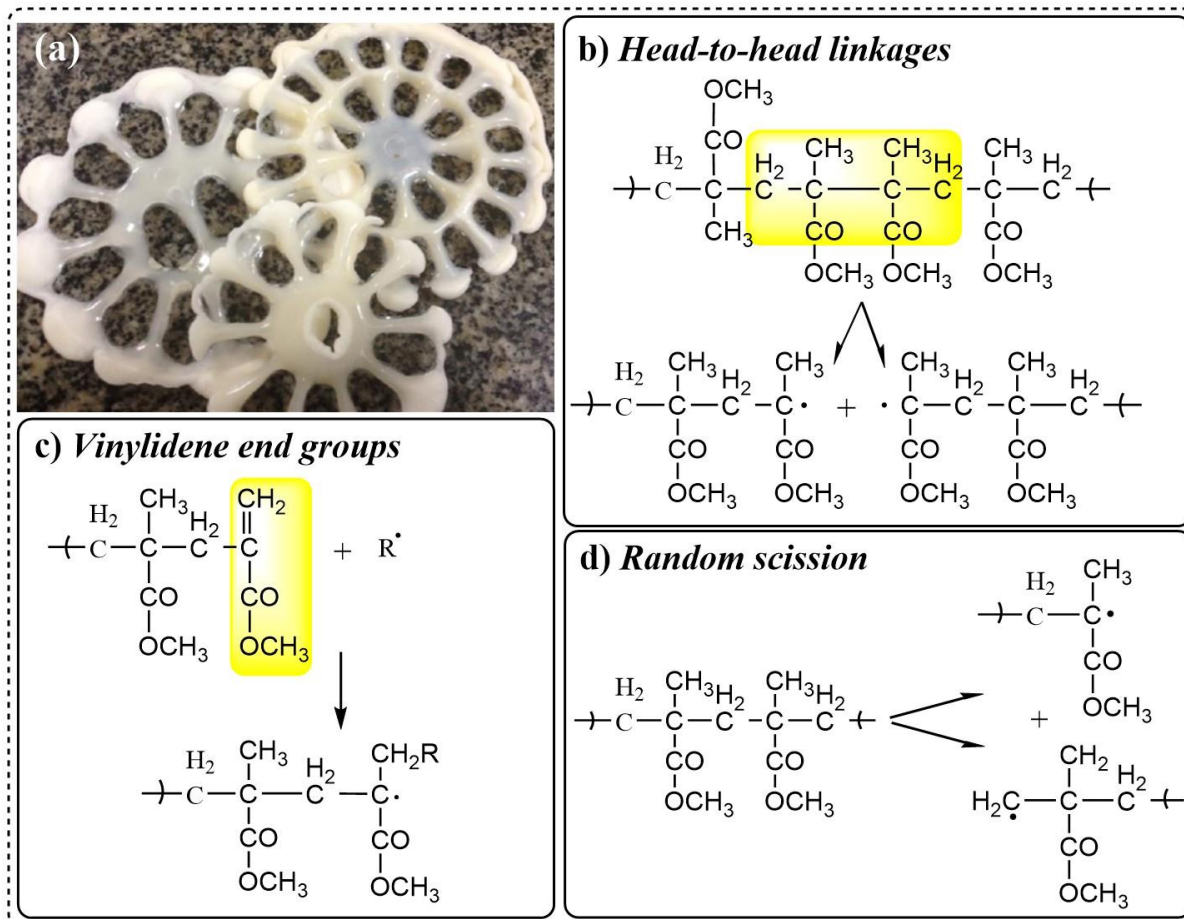
Fig. 1.1 – EGDMA crosslinked PMMA dental waste (a) and generally accepted initiation steps of the PMMA depolymerisation: breakage of head-to-head linkages (b), chain scission involving vinylidene end groups (c) and random main chain scissions (d) [20,22,23,27].

The proposed degradation steps have been supported by non-isothermal thermogravimetric analysis (TGA) [7,27,28]. For example, a model composed by four independent reaction steps and fifteen kinetic parameters has been reported to explain the thermal pyrolysis of PMMA prepared by free radical polymerisation [27]. In contrast, a model comprising four consecutive reaction steps and sixteen kinetic parameters has been proposed to explain the thermal degradation of PMMA under inert and oxidising environments [28].

However, the crosslinking effect on the PMMA depolymerisation kinetics has not been fully characterised, although some studies indicate a higher thermal stability associated to

6

crosslinked PMMA [25]. In addition, it is important to note that even though TGA experiments are a powerful tool for kinetic characterisation of chemical reactions [29], kinetics parameters and the evaluation of their statistical significance are scarcely reported [7,25,28], impairing the discrimination among reaction mechanisms [30,31].

Thus, this work presents the modelling of the depolymerisation kinetics involved in the thermal pyrolysis of ethylene glycol dimethacrylate (EGDMA) crosslinked PMMA from industrial dental waste for the first time. Kinetics parameters and their statistical significance have been determined by using eight non-isothermal TGA experiments with heating rates varying between 5 and 50 °C·min^{-1}. Our analysis indicates that the mechanism of depolymerisation of EGDMA crosslinked PMMA is likely to involve a consecutive reaction pathway involving two steps. The developed kinetic model - containing five kinetic parameters only - was able to predict well all non-isothermal TGA runs, and was validated against isothermal TGA experiments at 400 °C.

2. Materials and Methods

2.1 Materials

PMMA-based artificial teeth scraps produced by a dental industry, as illustrated in the Fig. 1.1(a), were studied in its original form, with pieces diameters ranging from 1 to 10 mm. The PMMA waste samples contained 1 wt.% of titanium oxide (TiO$_2$) and around 5 wt.% of the cross-linking agent ethylene glycol dimethacrylate (EGDMA), as described elsewhere [17]. For comparison, a homopolymer PMMA powder with particle average size below 200 μm produced by the same industry was also evaluated.

2.2 Thermogravimetric Experiments

Non-isothermal thermogravimetric analysis of the PMMA scraps was performed in a TGA STA 6000 equipment (Mettler Toledo, Ohio, USA), under nitrogen flow (20 mL·min^{-1}), at heating rates of 5, 10, 15, 25 and 50 °C·min^{-1}. Samples (~10 mg) were heated from 50 to 650 °C and kept at the final temperature for 5 min. In order to confirm the reproducibility of the thermogravimetric runs, four replicates were performed at the heating rate of 5 °C·min^{-1}.

Isothermal thermogravimetric analysis of the PMMA scraps was performed as described above at 300, 350 and 450 °C. Samples were heated from 50 °C to the final temperature with a heating rate of 100 °C·min^{-1} and kept at the final temperature for 4.5 h.

2.3 Mathematical Modelling of PMMA Kinetics of Depolymerisation

The aluminium sample holder was modelled as a batch reactor for the solid phase, as the atmospheric composition just above the crucible was kept essentially constant by the inert gas flow. The kinetics of depolymerisation was investigated by using two different modelling approaches, involving up to three irreversible reaction steps. In the first approach, independent reactions were described assuming a first-order rate for the polymer mass, whereas consecutive steps were considered in the second approach, Table 2.1.

Table 2.1 – Elementary reactions considered in the EGDMA crosslinked PMMA thermal depolymerisation.

Independent reactions		Consecutive reactions	
$P_1 \xrightarrow{\ k_1\ } V$	(a1)	$P_1 \xrightarrow{\ k_1\ } P_2 + V$	(b1)
$P_2 \xrightarrow{\ k_2\ } V$	(a2)	$P_2 \xrightarrow{\ k_2\ } P_3 + V$	(b2)
$P_3 \xrightarrow{\ k_3\ } V$	(a3)	$P_3 \xrightarrow{\ k_3\ } V$	(b3)

Thus, the independent reaction network assumed the simultaneous depolymerisation of different polymer chains into volatiles species (V). In contrast, the consecutive reaction mechanism assumed the formation of intermediary polymer species which undergo further depolymerisation.

The consumption rate of an elementary step in the solid phase was calculated through the law of mass action according to Eq. (2.1), where k_j is the rate constant of reaction j and P_i is the mass of polymer chains of type i.

$$r_j = k_j P_{i=j} \tag{2.1}$$

The net reaction rate was calculated in accordance to Eq. (2.2), where NR is the number of reactions considered in the global model (from 1 to 3) and $v_{i,j}$ is the stoichiometric coefficient of the component i in the reaction j, negative for the reactant and positive for the product.

$$R_i = \sum_{j=1}^{NR} v_{j,i} r_j \tag{2.2}$$

The mass of the polymer chains of type i, P_i, was normalised by the initial mass of the polymer, P_0, resulting in the system of ordinary differential equations represented by Eq. (2.3-2.4), where ε_i is the mass fraction of polymer chains of type i, P is the total mass of polymer at any time, and NP is the number of different types of polymer chains considered (from 1 to 3).

$$\frac{d\varepsilon_i}{dt} = R_i \tag{2.3}$$

$$\frac{dP}{dt} = P_0 \sum_{i=1}^{NP} \frac{d\varepsilon_i}{dt} \tag{2.4}$$

The dependence of the reaction rate constant, k_j, towards temperature was described by the reparameterised Arrhenius equation, Eq. (2.5) [32,33]. In Eq. (2.5), T is the measured temperature, and T_{ref} was defined as equal to 325 °C.

$$k_j = \exp\left(A_{Tref,j} + B_j \left(\frac{T - T_{ref}}{T} \right) \right) \tag{2.5}$$

The A_{Tref} constant is related to the pre-exponential factor of the original Arrhenius equation, k_0, according to Eq. (2.6) and B_j relates to the activation energy, E, according to Eq. (2.7).

$$A_{Tref,j} = \ln(k_{0,j}) - \frac{E_j}{R \cdot T_{ref}} \tag{2.6}$$

$$B_j = \frac{E_j}{R \cdot T_{ref}} \tag{2.7}$$

The number of reactions in the independent and consecutive modelling approaches, Table 2.1, was varied from one to three during the model development process, resulting in five different kinetic models that were tested against the experimental data. Thus, the number of kinetic optimization variables was equal to six when three reactions were considered ($A_{Tref,1}$, B_1, $A_{Tref,2}$, B_2, $A_{Tref,3}$, B_3), equal to four when two reactions were considered ($A_{Tref,1}$, B_1, $A_{Tref,2}$, B_2) and equal to two when only one reaction was evaluated ($A_{Tref,1}$, B_1). Additionally, for both modelling approaches, NP-1 mass fractions were estimated as initial condition for the ordinary differential equations, Eq. (2.3), being the sum of all mass fractions, at any time, equal to 1. The initial mass of the polymer, P_0, was also estimated, resulting in a total of $2 \cdot NR + NR$ parameters which were estimated from experimental data. Thus, for the modelling approach involving consecutive reactions, all initial mass fractions were allowed to be different from

zero, implying that the initial polymer could already contain degraded chains at the beginning of pyrolysis. Finally, it should also be noted that the heating rate was not explicitly presented in the model equations because the temperature used in the model calculations was the actual measured value [29,34].

2.5 Parameter Estimation

The ordinary differential equations were solved numerically using the backward differentiation technique available in DASSL code [35], with relative and absolute tolerances equal to 10^{-5}. The parameter estimation procedure consisted in the search of the best set of parameter estimates, θ, throughout the minimisation of the least-squares objective function, F_{obj}, Eq. (2.8). In the Eq. (2.8), NE is the number of experimental data points, P_i^{exp} denotes the experimental mass recorded during the thermogravimetric run, P_i^{mod} is the value calculated using Eq. (2.4), and x_i^{mod} represents the experimental condition of time and temperature.

$$F_{obj} = \sum_{i=1}^{NE} (P_i^{exp} - P_i^{mod}(x_i^{mod}, \theta))^2 \tag{2.8}$$

The minimisation of Eq. (2.8) was performed using a hybrid optimisation method implemented in Fortran 90, in which the Particle Swarm Optimization algorithm [36] is used in the initial phase of minimisation [37,38]. The best estimate of the point of the minimum is used as an initial guess for a second estimation round, using the Gauss-Newton method [31,39]. Thirty particles were used, and at least 1000 iterations were performed, resulting in at least 30000 evaluations of the objective function. Convergence was achieved when the relative modification of the objective function was smaller than 1.0×10^{-6}. Statistical significance of model parameters was evaluated with the standard t-test [40], with 95 % confidence level. The evaluation of the model adequacy was performed by comparing models prediction variance,

σ_m^2, as defined in accordance to Eq. (2.9), with the help of the standard F-test [31,40]. In Eq. (2.9), F_{obj} is the value of the objective function at its point of minimum, NE is the number of experimental data points and $NPar$ is the number of parameters estimated for the model m.

$$\sigma_m^2 = \frac{F_{obj}}{\left(NE - NPar\right)} \tag{2.9}$$

2.4 Experimental Data Treatment

To reduce the computational effort required for the minimisation of the objective function during the parameter estimation procedure, in this work, the experimental data was sampled as recommended by Conesa *et al.* (2001) [34]. This procedure was found necessary due to the high recording frequency of the TGA instrument, which resulted in thermograms containing up to 45000 data points per experiment, depending on the heating rate. Thus, typically, the sampling procedure applied collected 1 data point for every 5 in the thermogram regions of small and slow weight loss (up to nearly 200 °C) and it collected 3 data points for every 5 in the range of fast weight loss (above 200 °C), as it is illustrated in the Fig. S1 of the *Supporting Information (SI)*.

3. Results and Discussion

The good reproducibility of the thermogravimetric runs was confirmed by four identical experiments performed using the EGDMA crosslinked PMMA scraps with heating rates equal to 5 °C·min^{-1}, as illustrated in the Fig. 3.1. For comparison, the thermogravimetric profile of the homopolymer PMMA is also shown.
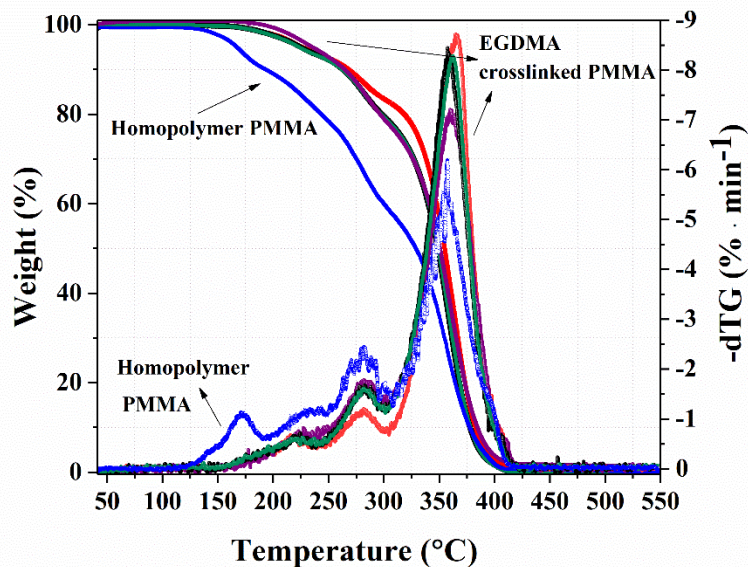
Fig. 3.1 – Replicates of TGA thermogravimetric thermograms for the EGDMA crosslinked (●, ●, ●, ●) and homopolymer PMMA (●) at 5 °C·min^{-1}.

As expected, the EGDMA crosslinked PMMA exhibited a higher thermal stability in comparison to its counterpart homopolymer, with main weight loss processes being observed above 200 °C. Moreover, up to three degradation processes could be associated to the weight loss steps, as suggested by the presence of three points of maximum in the thermogram derivative, illustrated in the Fig. 3.1 (right Y-axis). In contrast, the homopolymer PMMA started to degrade around 150 °C and presented a distinct thermogram profile, in which four points of maximum could be observed in the thermogram derivative, suggesting the presence of up to four processes of degradation, as also observed by other authors [27].

As discussed previously, the PMMA depolymerisation steps may involve the breakdown of head-to-head linkages, chain scissions associated to vinylidene end groups, random main chain scissions, methoxycarbonyl side groups scissions and cross-linking points scission, depending on the polymer structure [20,22,24,25]. For the EGDMA crosslinked PMMA dental waste investigated in this work, whereas the main degradation process could be associated to main chain random scissions, which could also involve methoxycarbonyl side

groups scissions, the processes observed at lower temperatures could be associated to the combined effect of different degradation steps, which could involve scissions of cross-linking points and chain scissions associated with vinylidene end groups. Therefore, it was an objective of this study to develop a kinetic model able to predict the depolymerisation kinetics of EGDMA crosslinked PMMA. To achieve this, two modelling approaches were investigated, as illustrated in Table 2.1 from *Section 2.3*. In the first modelling approach, up to three independent reactions were evaluated [7,25,27], while in the second, up to three consecutive and dependent reactions were considered [7,28]. Each model was fitted to the experimental data and the statistical significance of the estimative parameters was assessed.

3.1 The Three Degradation Reaction Steps Models

The use of a three degradation reaction steps model (in both modelling approaches) resulted in a good fit of the experimental data, with linear correlation coefficients always higher than 0.99, as it is illustrated in Fig. S2 of the *SI*. Nevertheless, in both cases, some of the kinetic parameters were verified to present no statistical significance, indicating that the evaluated models could be overparameterised and that the hypothesis of a depolymerisation process involving three degradation reaction steps, as described by Eq. (2.1-2.4), could be unrealistic. It should be noted that the total number of parameters estimated from experimental data when three degradation steps were considered was equal to nine for both modelling approaches. The finding that some of these parameters were not statistically significant is very surprising, since up to sixteen kinetic parameters have been used to explain the depolymerisation kinetics of PMMA prepared by free radical polymerisation [27,28]. Thus, it is possible to conclude that the depolymerisation kinetics of EGDMA crosslinked PMMA should be distinct from its counterpart pure homopolymer, as it is indeed the case indicated by our experiments, Fig. 3.1.

3.2 The Two Degradation Reaction Steps Models

When a two degradation reaction steps model was evaluated, both modelling approaches were able to represent well the experimental data and all kinetic parameters were found to be statistically meaningful, as it is illustrated in the Fig. 3.2 and Table 3.1 for the consecutive reaction modelling approach.
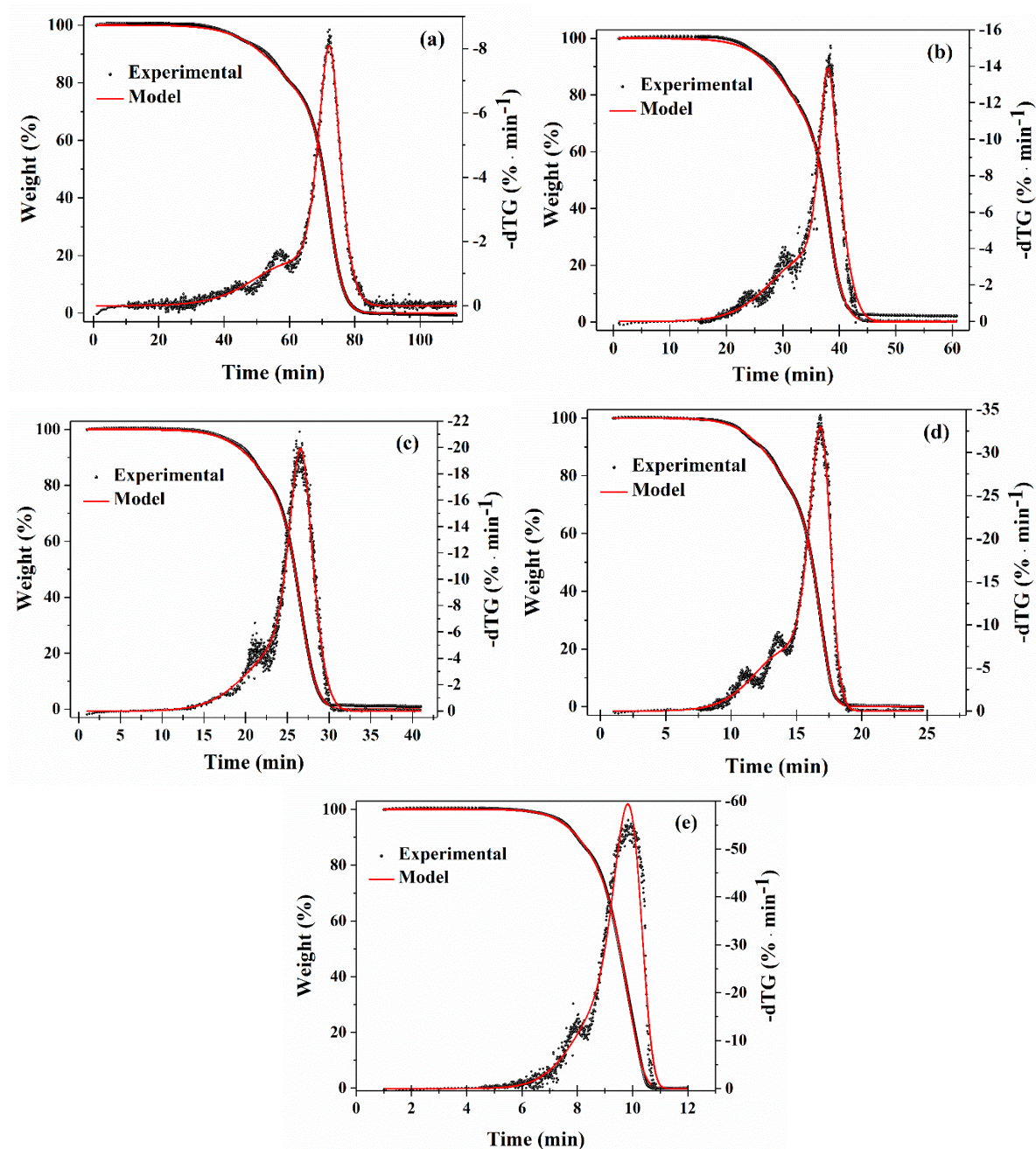
Fig. 3.2 – Experimental thermogravimetric profiles (●) and the two consecutive degradation steps model (—) at the heating rates equal to 5 (a), 10 (b), 15 (c), 25 (d) and 50 (e) °C·min^{-1}. Kinetics parameters are summarised in Table 3.1.

However, the evaluation of the parameter estimates demonstrated that the hypothesis of a two independent degradation reaction steps led to kinetic estimates highly correlated with the heating rate, while that much smaller correlations could be verified for kinetic parameters estimated considering the two consecutive reactions model, as it is illustrated in the Fig. 3.3. For instance, the linear correlation coefficient, ρ, between the kinetic parameter estimate $A_{Tref,1}$ and the heating rate could be calculated as equal to 0.99 while considering the independent reaction modelling approach and as equal to 0.52 when considering the consecutive reaction model, Fig. 3.3 (a).

Whereas the effect of heating rate on the kinetic parameter estimates may indicate that heat transfer processes influenced the pyrolysis kinetics [34], it can be suggested that the appropriate choice of the kinetic reaction pathway may minimise the influence of heat transfer effects on the obtained kinetic parameters.
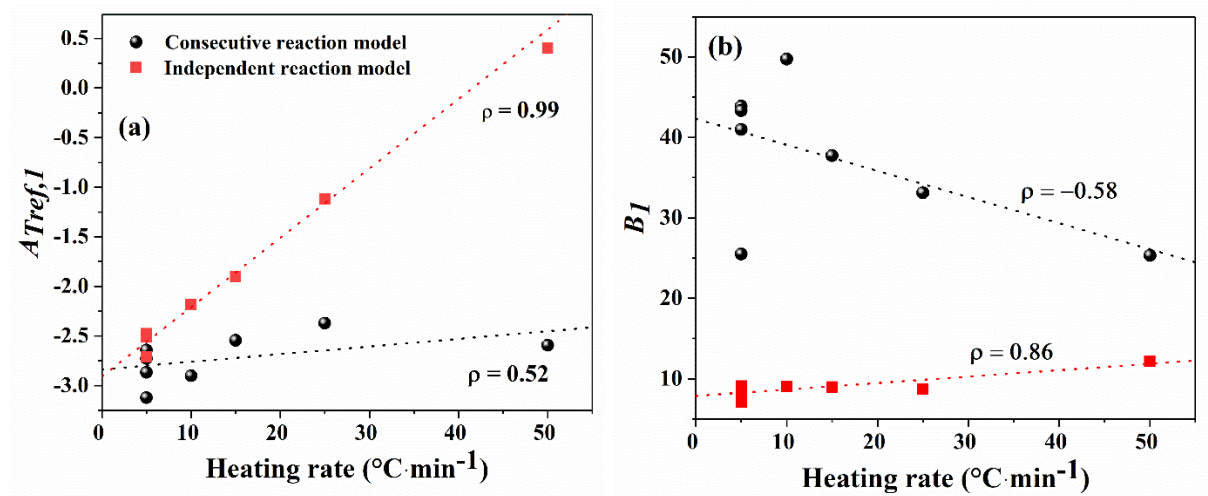
Table 3.1 also presents the initial mass fraction and polymer mass which were estimated from the experimental data for the consecutive reaction modelling approach. The initial mass estimated represented very well the initial experimental mass used in the TGA runs, as it is illustrated in Fig. 3.2. In addition, the initial mass fraction of polymer chains, as calculated by considering the two consecutive degradation steps model, indicated that up to 30 wt.%, in average, of polymer chains could already be degraded to some extent before the start of pyrolysis. As observed for the kinetic parameters, the two consecutive reactions model allowed for the estimation of initial mass fractions which were not correlated to the heating rate, in

contrast to the mass fractions estimated by using the independent reaction model, which demonstrated significant correlation with the heating rate, as it is illustrated in the Fig. 3.3 (e).

Table 3.1 – Kinetic parameters estimates and their standard deviations obtained from experimental thermograms for the two consecutive degradation steps model.

Exp.	β [a]	$A_{Tref,1}$	B_1	$A_{Tref,2}$	B_2	$\varepsilon_{1,0}$	P_0 (mg)
1	5	-3.12 ± 0.01	25.51 ± 0.19	-0.52 ± 0.09	14.09 ± 0.34	0.79 ± 0.004	6.09
2	5	-2.73 ± 0.005	40.97 ± 0.33	-1.74 ± 0.007	10.31 ± 0.02	0.70 ± 0.002	8.60
3	5	-2.87 ± 0.006	43.86 ± 0.33	-1.76 ± 0.006	9.25 ± 0.03	0.77 ± 0.001	11.22
4	5	-2.64 ± 0.006	43.34 ± 0.41	-1.77 ± 0.007	10.43 ± 0.03	0.69 ± 0.002	6.76
5	10	-2.90 ± 0.04	49.73 ± 1.27	-1.61 ± 0.01	10.64 ± 0.06	0.58 ± 0.004	7.20
6	15	-2.54 ± 0.03	37.72 ± 0.69	-1.40 ± 0.01	11.31 ± 0.09	0.64 ± 0.006	11.13
7	25	-2.37 ± 0.01	33.12 ± 0.31	-0.40 ± 0.01	10.65 ± 0.04	0.68 ± 0.003	10.61
8	50	-2.60 ± 0.04	25.32 ± 0.28	-0.25 ± 0.12	14.11 ± 0.38	0.77 ± 0.02	10.68
Average		-2.72 ± 0.24	37.44 ± 8.84	-1.18 ± 0.67	11.35 ± 1.79	0.70 ± 0.07	

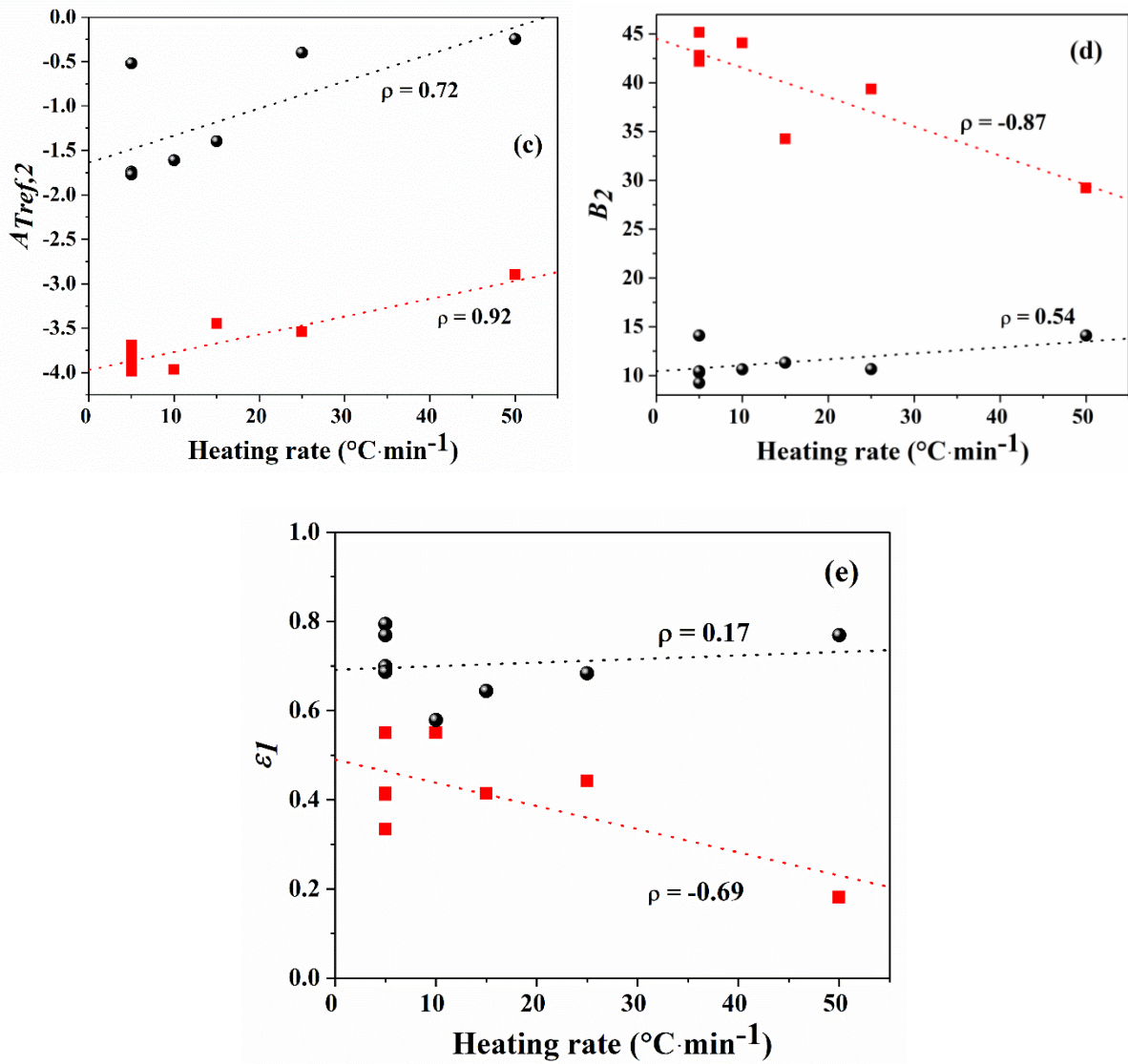[a] Heating rate (in $°C \cdot min^{-1}$).

Fig. 3.3 - Linear correlation relationship between the kinetic parameter $A_{Tref,1}$ (a), B_1 (b), $A_{Tref,2}$ (c), B_2 (d), the initial mass fraction, ε_1, (e), and the heating rate for the independent (■) and consecutive (●) reactions model approaches. Note how linear correlation coefficients (ρ) are always lower when the two consecutive degradation steps model is considered.

From the average values presented in Table 3.1, the activation energy and the pre-exponential values were calculated with the help of Eq. (2.6-2.7) and their values are presented in Table 3.2.

Table 3.2 – Activation energies and pre-exponential factors calculated from kinetic parameter estimates for the two consecutive degradation steps model of EGDMA crosslinked PMMA pyrolysis.

	E (kJ·mol^{-1})	k_0 (min^{-1})
Depolymerisation reaction (b1) $$P_1 \xrightarrow{k_1} P_2 + V$$	186.21	2.01 x 10^{13}
Depolymerisation reaction (b2) $$P_2 \xrightarrow{k_2} P_3 + V$$	56.44	4.35 x 10^2

The activation energy for the random scission depolymerisation step of PMMA pyrolysis has been reported as equal to ~200 [27], 210 [41] and 161 kJ·mol^{-1} [28], whereas the end-chain scission activation energy has been reported as equal to 154 kJ·mol^{-1} [21]. Thus, it can be suggested that the crosslinking agent may reduce the activation energy of one of the degradation steps in the case of the EGDMA crosslinked PMMA pyrolysis.

Finally, it should be noted that despite the presence of 1 wt.% of TiO$_2$ in the EGDMA crosslinked PMMA dental waste, which is used as a reinforcement agent for improving mechanical properties of the dental PMMA resin [42], no catalytic effect of TiO$_2$ on the depolymerisation kinetics has been observed, as indicated by the thermogravimetric analysis of EGDMA crosslinked PMMA containing no TiO$_2$ [43,44], Fig. S4 in the *SI,* and by the kinetic parameters estimated from the above experimental data for the two consecutive degradation steps model, Table S1 in the *SI*.

3.3 The One Degradation Step Model

The hypothesis of only one degradation reaction step, involving the depolymerisation of polymer chains P_i into volatiles, was also investigated. In this case, modelling approaches become the same, and the number of parameters which require estimation from experimental

data is equal to three ($A_{Tref,1}$, B_1 and the initial condition of the ordinary differential equation). The fitting of this model to the thermograms obtained at the different heating rates also resulted in high linear correlation coefficients between experimental data and model predictions, always higher than 0.99, indicating a good fit. However, the comparison of the model prediction variance between the different models, that is, the model containing one degradation step and the model containing two consecutive degradation steps, with the help of the standard test-F [31,39,40], indicates a significant loss of quality fit when only one degradation step is considered. Thus, the modelling approach involving two consecutive reaction steps seems to be the most promising to represent the pyrolysis of EGDMA crosslinked PMMA.

3.4 Simulation and Model Validation

Fig. 3.4 shows the conversion as a function of pyrolysis time calculated by the simulation of the two consecutive degradation steps model at different temperatures.
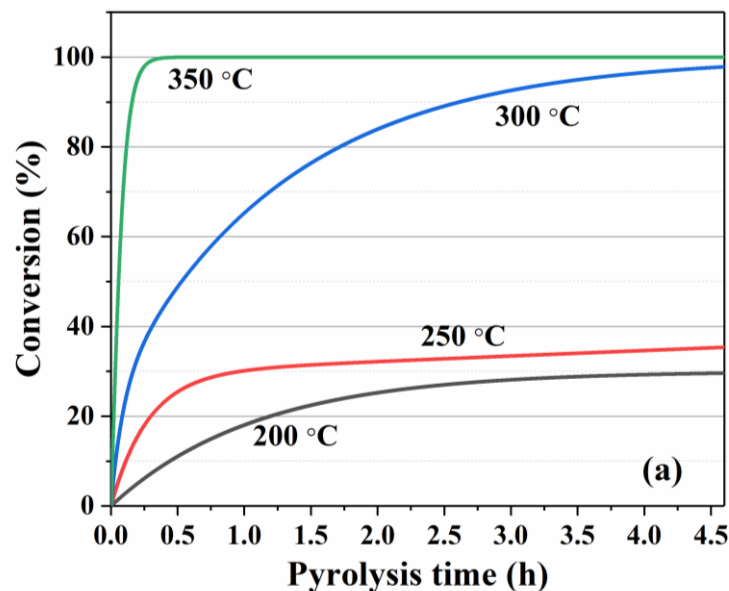

Fig. 3.4 – Simulation of EGDMA crosslinked PMMA pyrolysis conversion as a function of time at 200, 250, 300, and 350 °C.

As expected, the model indicates that the amount of depolymerised PMMA increases as a function of time and temperature. Moreover, the conversion reaches a plateau at around 30 % at temperatures between 200 and 250 °C, indicating that higher temperatures are required for the complete pyrolysis conversion of EGDMA crosslinked PMMA, in line with thermograms presented in Fig. 3.1 and previous findings from Braido *et al* (2018) [17].

For the validation of the two consecutive degradation steps model, isothermal TGA experiments were carried out at 300, 350 and 400 °C, as described in the Section 2.2. Additionally, mass conversions reported by Braido *et al* (2018) [17], who investigated the thermal pyrolysis of EGDMA crosslinked PMMA dental waste at isothermal conditions using a larger scale of 30 g, were further used to assess the system behaviour. Table 3.3 compares the experimental mass conversions obtained from the isothermal TGA runs performed in this work with the values obtained for the larger scale process (from [17]), after 1, 1.5 and 2 h of isothermal processing at different temperatures. Full experimental isothermal thermograms are presented in the Fig. S3 of the *SI*.

Table 3.3 – Experimental mass conversion, *X*, (in %) for the isothermal pyrolysis of EGDMA crosslinked PMMA at 300, 350 and 400 °C.

	Pyrolysis Temperature (°C)					
Scale	300		350		400	
	Time (h)	*X (%)*	*Time (h)*	*X (%)*	*Time (h)*	*X (%)*
10 mg	1	64.66	1.5	98.67	1	100
10 mg	2	73.20				
30 g [a]	1	38.99 [a]	1.5	72.70 [a]	1	96.71 [a]
30 g [a]	2	33.80 [a]			2	99.08 [a]

[a] Data from Braido *et al* (2018) [17].

Conversions reported for the larger scale process were significantly smaller than the ones obtained in the isothermal TGA experiments at 300 and 350 °C, suggesting that thermal effects may play an important role in the EGDMA crosslinked PMMA pyrolysis at these lower temperatures. In contrast, experimental mass conversions obtained at 400 °C demonstrated a better agreement between the two process scales, suggesting that at this higher temperature the pyrolysis kinetics may be favoured, reducing the importance of thermal effects.

As the two consecutive degradation steps model developed in this work assumes uniform chemical composition and energy distribution within the solid dental waste under pyrolysis, that is, a system with no mass or energy transfer constraints, we have used the isothermal TGA experimental data obtained at 400 °C for the model validation. Fig. 3.5(a) illustrates the excellent agreement between the two consecutive degradation steps model predictions and the isothermal experimental data at 400 °C. Fig.3.5(b) further presents the absolute differences between simulated and experimentally observed mass conversions, ΔX, from the isothermal TGA experiments. Whereas the model overestimates mass conversions at 300 °C, the absolute difference between calculated and observed mass conversions is exponentially decreased from 6.41 to 0.43 % as a function of pyrolysis time at 350 °C, and is zero at 400 °C, emphasising the increased model ability for describing the EGDMA crosslinked PMMA pyrolysis as temperature increases from 300 to 400 °C.

Therefore, whereas model simulations presented in Fig 3.4 explains the two consecutive degradation steps model behaviour, its application towards larger industrial scales may require the consideration of energy transfer constraints, in particular for process temperatures lower than 400 °C.
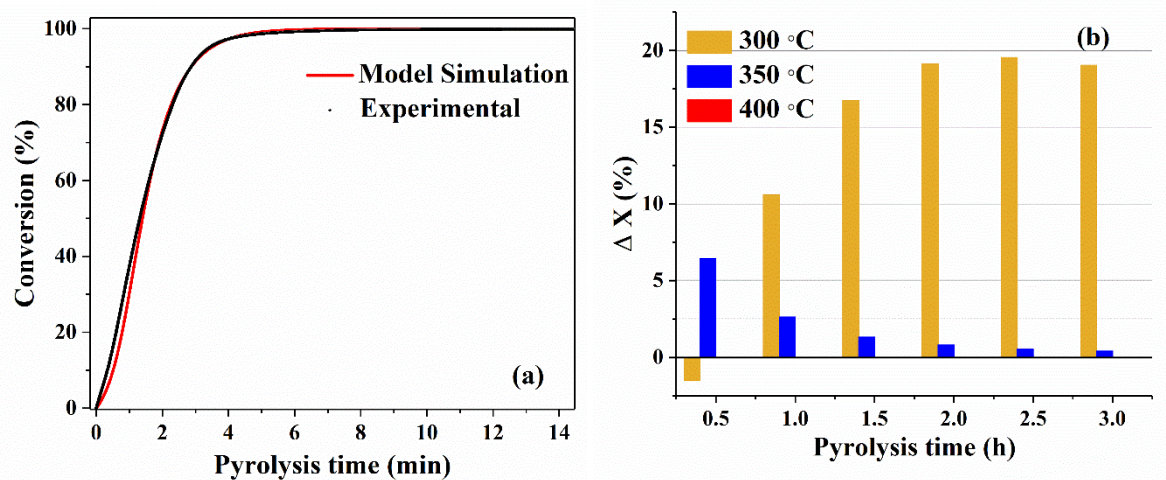
Fig. 3.5 – Simulation and isothermal TGA experimental data of the EGDMA crosslinked PMMA pyrolysis conversion as a function of time at 400 °C (a) and absolute differences between model prediction and experimental mass conversions, ΔX, obtained by isothermal TGA experiments as a function of time at 300, 350 and 400 °C (b).

4. Conclusions

This work has presented the modelling of the depolymerisation kinetics involved in the thermal pyrolysis of ethylene glycol dimethacrylate (EGDMA) crosslinked PMMA from industrial dental waste for the first time. Kinetics parameters and their statistical significance have been determined by using eight non-isothermal TGA experiments with heating rates varying between 5 and 50 °C/min. Our analysis indicates that the mechanism of depolymerisation of EGDMA crosslinked PMMA is likely to follow a consecutive reaction pathway involving two steps, since this hypothesis allowed for the estimation of kinetic parameters presenting low or non-significant linear correlation coefficients with the heating rate. Therefore, it has been shown that the kinetic model structure may contribute for minimising heat transfer effects on the estimated kinetic parameters. The developed kinetic model - containing five kinetic parameters only - was able to predict well all non-isothermal TGA runs, and was validated against isothermal TGA experiments at 400 °C.

5. Acknowledgements

6. References

[1]   A. Quye, Quality Matters for Historical Plastics: The Past-Making of Cellulose Nitrates for Future Preservation, Cah. François Viète. 2 (2017) 45–65.

[2]   R. Geyer, J.R. Jambeck, K.L. Law, Production, uses, and fate of all plastics ever made, Sci. Adv. 3 (2017) 5. doi:10.1126/sciadv.1700782.

[3]   A. Rahimi, J.M. García, Chemical recycling of waste plastics for new materials production, Nat. Rev. Chem. 1 (2017) 0046. doi:10.1038/s41570-017-0046.

[4]   PlasticsEurope, Plastics-the Facts 2017, https://www.plasticseurope.org, 2018 (Accessed 06 August 2018).

[5]   S. Kumar, A.K. Panda, R.K. Singh, A review on tertiary recycling of high-density polyethylene to fuel, Resour. Conserv. Recycl. 55 (2011) 893–910. doi:10.1016/j.resconrec.2011.05.005.

[6]   ASTM International, Standard Guide for Development of ASTM Standards Relating to Recycling and Use of Recycled Plastics, D 5033 (2000) 1–6.

[7]   B.F. Sasse, G. Emig, Chemical Recycling of Polymer Materials, Chem. Eng. Technol. 21 (1998) 777–789. doi:10.1002/(SICI)1521-4125(199810)21:10<777::AID-

CEAT777>3.0.CO;2-L.

[8]   E. Esmizadeh, S. Khalili, A. Vahidifar, G. Naderi, C. Dubois, Waste Polymethyl
        Methacrylate (PMMA): Recycling and high-yield monomer recovery, in: M. L., K. O.,
        K. B. (Eds.), Handb. Ecomater., Springer, 2018: pp. 1–33. doi:10.1007/978-3-319-
        68255-6_164.

[9]   Y. Kikuchi, M. Hirao, T. Ookubo, A. Sasaki, Design of recycling system for
        poly(methyl methacrylate) (PMMA). Part 1: Recycling scenario analysis, Int. J. Life
        Cycle Assess. 19 (2014) 120–129. doi:10.1007/s11367-013-0624-y.

[10]   G. Odian, Principles of Polymerization, 4º, Wiley-Interscience, New York, 2004.
        doi:10.1017/CBO9780511813535.

[11]   G. Lopez, M. Artetxe, M. Amutio, G. Elordi, R. Aguado, M. Olazar, J. Bilbao,
        Recycling poly-(methyl methacrylate) by pyrolysis in a conical spouted bed reactor,
        Chem. Eng. Process. Process Intensif. 49 (2010) 1089–1094.
        doi:10.1016/j.cep.2010.08.002.

[12]   U. Ali, K.J.B.A. Karim, N.A. Buang, A Review of the Properties and Applications of
        Poly (Methyl Methacrylate) (PMMA), Polym. Rev. 55 (2015) 678–705.
        doi:10.1080/15583724.2015.1031377.

[13]   K. Charmondusit, L. Seeluangsawat, Recycling of poly(methyl methacrylate) scrap in
        the styrene-methyl methacrylate copolymer cast sheet process, Resour. Conserv.
        Recycl. 54 (2009) 97–103. doi:10.1016/j.resconrec.2009.07.005.

[14]   A.Z.V. E. ŠuŠterŠic, M. TuŠsar, Asphalt concrete modification with waste
        PMMA/ATH, Mater. Struct. 47 (2014) 1817–1824. doi:DOI 10.1617/s11527-013-
        0152-z.

[15]   S.S. Suresh, S. Mohanty, S.K. Nayak, Investigation into the mechanical and thermal properties of poly(methyl methacrylate) recovered from light guidance panels with a focus on future remanufacturing and sustainable waste management, J. Remanufacturing. 7 (2017) 217–233. doi:10.1007/s13243-017-0041-7.

[16]   A.R. Prado, A.G. Leal-Junior, C. Marques, S. Leite, G.L. de Sena, L.C. Machado, A. Frizera, M.R.N. Ribeiro, M.J. Pontes, Polymethyl methacrylate (PMMA) recycling for the production of optical fiber sensor systems, Opt. Express. 25 (2017) 30051–30060. doi:10.1364/oe.25.030051.

[17]   R.S. Braido, L.E.P. Borges, J.C. Pinto, Chemical recycling of crosslinked poly(methyl methacrylate) and characterization of polymers produced with the recycled monomer, J. Anal. Appl. Pyrolysis. 132 (2018) 47–55. doi:10.1016/j.jaap.2018.03.017.

[18]   D.S. Achilias, Chemical recycling of poly(methyl methacrylate) by pyrolysis. Potential use of the liquid fraction as a raw material for the reproduction of the polymer, Eur. Polym. J. 43 (2007) 2564–2575. doi:10.1016/j.eurpolymj.2007.02.044.

[19]   W. Kaminsky, C. Eger, Pyrolysis of filled PMMA for monomer recovery, J. Anal. Appl. Pyrolysis. 58–59 (2001) 781–787. doi:10.1016/S0165-2370(00)00171-6.

[20]   T. Kashiwagi, A. Inaba, J.E. Brown, K. Hatada, T. Kitayama, E. Masuda, Effects of Weak Linkages on the Thermal and Oxidative Degradation of Poly (methyl methacrylates), Macromolecules. 19 (1986) 2160–2168. doi:10.1021/ma00162a010.

[21]   L.E. Manring, Thermal Degradation of Saturated Poly(Methyl Methacrylate), Macromolecules. 21 (1988) 528–530. doi:10.1021/ma00180a046.

[22]   L.E. Manring, Thermal degradation of Poly(methyl methacrylate). 2. Vinyl-Terminated Polymer, Macromolecules. 22 (1989) 2673–2677.

doi:10.1021/ma00196a024.

[23] G.M. Manring, L.E., Sogah, D. Y., Cohen, Thermal degradation of Poly(methyl methacrylate). 3. Polymer with Head-to-Head Linkages, Macromolecules. 22 (1989) 4652–4654. doi:10.1021/ma00202a048.

[24] L.E. Manring, Thermal Degradation of Poly(methyl methacrylate). 4. Random Side-Group Scission, Macromolecules. 24 (1991) 3304–3309. doi:10.1021/ma00011a040.

[25] J. Rychlý, J. Pavlinec, Thermal degradation of free radically prepared poly(methyl methacrylate). A nonisothermal weight loss study, Polym. Degrad. Stab. 28 (1990) 1–15. doi:10.1016/0141-3910(90)90048-C.

[26] K. Min, M. Silberstein, N.R. Aluru, Crosslinking PMMA: Molecular dynamics investigation of the shear response, J. Polym. Sci. Part B Polym. Phys. 52 (2014) 444–449. doi:10.1002/polb.23437.

[27] M. Ferriol, A. Gentilhomme, M. Cochez, Thermal degradation of poly (methyl methacrylate)(PMMA): modelling of DTG and TG curves, Polym. Degrad. Stab. 79 (2003) 271–281. doi:10.1016/S0141-3910(02)00291-4.

[28] T. Fateh, F. Richard, T. Rogaume, P. Joseph, Experimental and modelling studies on the kinetics and mechanisms of thermal degradation of polymethyl methacrylate in nitrogen and air, J. Anal. Appl. Pyrolysis. 120 (2016) 423–433. doi:10.1016/j.jaap.2016.06.014.

[29] F.S. Toniolo, E. Barbosa-Coutinho, M. Schwaab, I.C.L. Leocadio, R.S. Aderne, M. Schmal, J.C. Pinto, Kinetics of the catalytic combustion of diesel soot with MoO_3/Al_2O_3 catalyst from thermogravimetric analyses, Appl. Catal. A Gen. 342 (2008) 87–92. doi:10.1016/j.apcata.2008.03.004.

[30] M. Schwaab, F.M. Silva, C.A. Queipo, A.G. Barreto, M. Nele, J.C. Pinto, A new approach for sequential experimental design for model discrimination, Chem. Eng. Sci. 61 (2006) 5791–5806. doi:10.1016/j.ces.2006.04.001.

[31] S. Da Ros, M. Schwaab, J.C. Pinto, Parameter Estimation and Statistical Methods, Ref. Modul. Chem. Mol. Sci. Chem. Eng. (2017). doi:10.1016/B978-0-12-409547-2.13918-6.

[32] M. Schwaab, J.C. Pinto, Optimum reference temperature for reparameterization of the Arrhenius equation. Part 1: Problems involving one kinetic constant, Chem. Eng. Sci. 62 (2007) 2750–2764. doi:10.1016/j.ces.2008.03.010.

[33] M. Schwaab, L.P. Lemos, J.C. Pinto, Optimum reference temperature for reparameterization of the Arrhenius equation. Part 2: Problems involving multiple reparameterizations, Chem. Eng. Sci. 63 (2008) 2895–2906. doi:10.1016/j.ces.2008.03.010.

[34] J.A. Conesa, A. Marcilla, J.A. Caballero, R. Font, Comments on the validity and utility of the different methods for kinetic analysis of thermogravimetric data, J. Anal. Appl. Pyrolysis. 58–59 (2001) 617–633. doi:10.1016/S0165-2370(00)00130-3.

[35] L.R. Petzold, A description of DASSL: A Differential/Algebraic system solver, in: IMACA World Congr., Montreal, 1982: pp. 1–11. doi:https://www.osti.gov/servlets/purl/5882821.

[36] R. Kennedy, J., Eberhart, Particle Swarm Optimization, in: Proc. IEEE Int. Conf. Neural Networks, Perth, 1995: pp. 1942–1948. doi:10.1007/978-3-319-93073-2_6.

[37] T.J.S. F. B. Noronha, J. C. Pinto, J. L. Monteiro, M. W. Lobao, ESTIMA: Um Pacote Computacional para Estimação de Parâmetros e Projeto de Experimentos, Rio de

Janeiro, 1993.

[38]   M. Schwaab, E.C. Biscaia, J.L. Monteiro, J.C. Pinto, Nonlinear parameter estimation through particle swarm optimization, Chem. Eng. Sci. 63 (2008) 1542–1552. doi:10.1016/j.ces.2007.11.024.

[39]   J.C.P. M. Schwaab, Analise de Dados Experimentais I - Fundamentos de Estatística e Estimação de Parâmetros, e-papers, Rio de Janeiro, 2007.

[40]   W.G. Box, G.P., Hunter, J.S., Hunter, Statistics for Experimenters - Design, Innovation, and Discovery, Second, Wiley-Interscience, John Wiley & Sons, Inc., New Jersey, 2005. doi:10.1017/S1742170510000062.

[41]   T. Hirata, T. Kashiwagi, J.E. Brown, Thermal and Oxidative Degradation of Poly(methyl methacrylate): Molecular Weight, Macromolecules. 18 (1985) 1410–1418. doi:10.1021/ma00144a003.

[42]   M.M. and R.A. Gad, Behavior of PMMA Denture Base Materials Containing Titanium Dioxide Nanoparticles : A Literature Review, Int. J. Biomater. 2019 (2019). doi:https://doi.org/10.1155/2019/6190610 Review.

[43]   T. Paiva, L. Vieira, P. Melo, M. Nele, J.C. Pinto, In Situ Incorporation of Praziquantel in Polymer Microparticles through Suspension Polymerization for Treatment of Schistosomiasis, Macromol. React. Eng. 13 (2019) 1–12. doi:10.1002/mren.201800064.

[44]   T.F. Paiva, Development of smart polymeric microparticles for the modified release of Praziquantel for the treatment of schistosomiasis, Federal University of Rio de Janeiro (UFRJ), 2019.